Supporting Information

Table S1. Reproducibility of BET Surface Area for 5Li-Ru/Al Catalyst (n=3)

Batch	specific surface area ($m^2 \cdot g^{-1}$)	pore volume ($cm^3 \cdot g^{-1}$)	pore size (nm)	note
1	229.8	0.23	4.1	Standard synthesis
2	225.6	0.25	4.3	New precursor batch
3	221.7	0.21	4.0	New precursor batch
Mean±SD	225.7±5.9	0.23±0.02	4.2±0.2	RSD=2.6%

Three independent syntheses demonstrated excellent reproducibility of the 5Li-Ru/Al catalyst, as evidenced by highly consistent surface area data (225.7±5.9 $m^2 \cdot g^{-1}$, RSD=2.6%). Although Batch 3 showed a slightly decreased surface area of 221.7 $m^2 \cdot g^{-1}$ due to precursor batch variation, the results still significantly outperform the 5% acceptance threshold for mesoporous materials. The minor variations in pore volume (0.23±0.02 $cm^3 \cdot g^{-1}$) and pore size (4.1±0.2 nm) further confirm the robustness of the synthesis protocol. This reproducibility ensures reliable material foundation for subsequent catalytic mechanism studies while indicating promising potential for industrial scale-up.

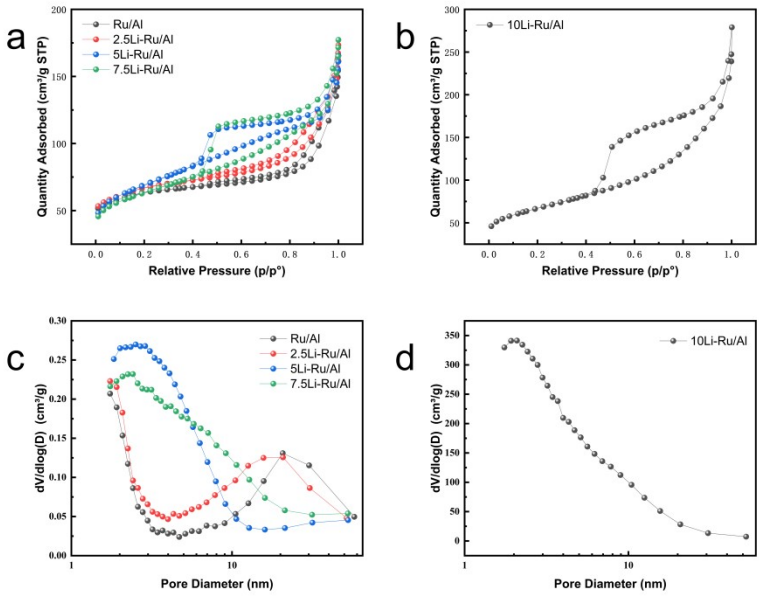

Figure S1 N_2 Adsorption-Desorption Isotherms and Pore Size Distributions of Ru-Based Catalysts

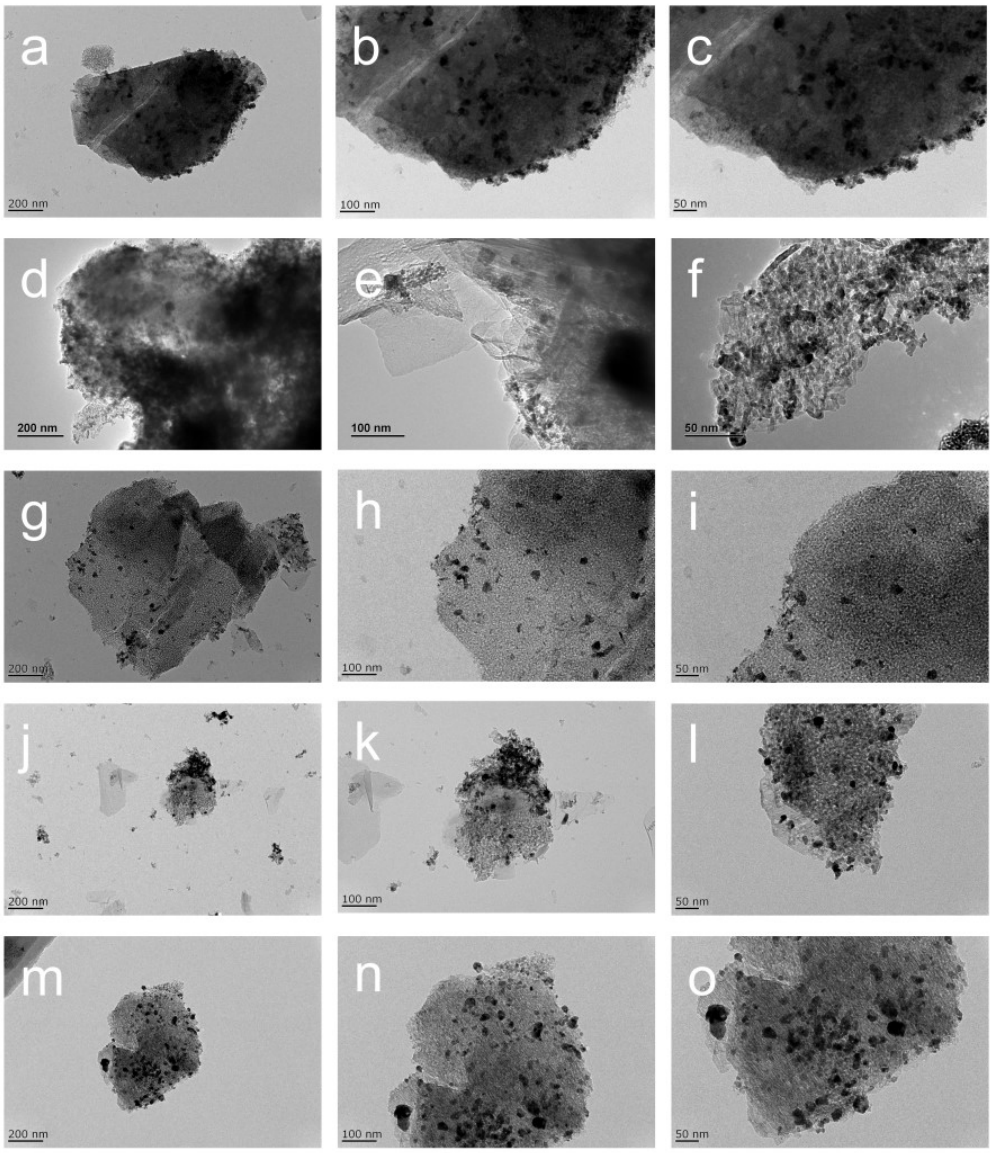

Figure S2. TEM images of Ru/Al and Li-modified Ru/Al catalysts
(a-c) Ru/Al, (d-f) 2.5Li-Ru/Al, (g-i) 5Li-Ru/Al, (j-l) 7.5Li-Ru/Al, (m-o) 10Li-Ru/Al

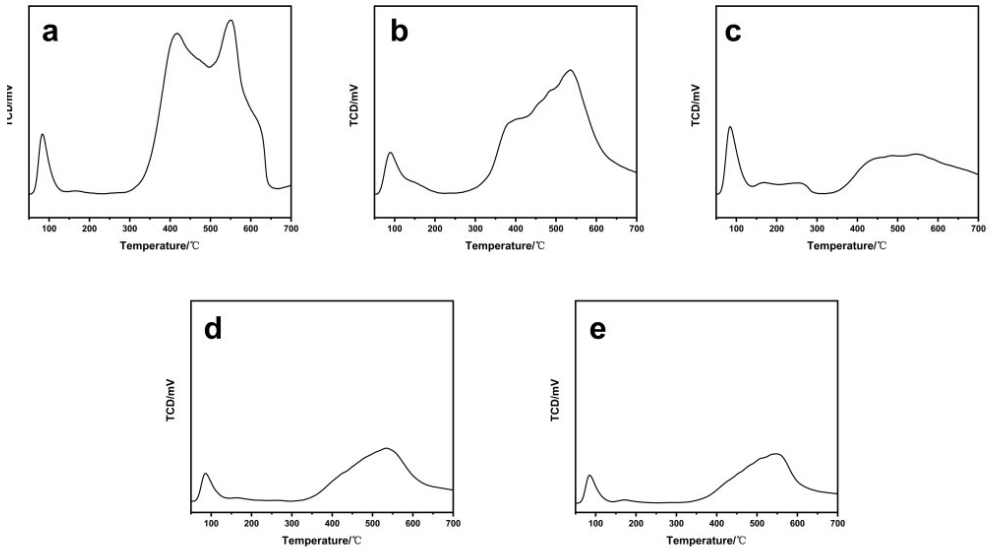

Figure S3. Ammonia temperature-programmed desorption (NH_3-TPD) profiles of (a) Ru/Al, (b) 2.5Li-Ru/Al, (c) 5Li-Ru/Al, (d) 7.5Li-Ru/Al, and (e) 10Li-Ru/Al catalysts

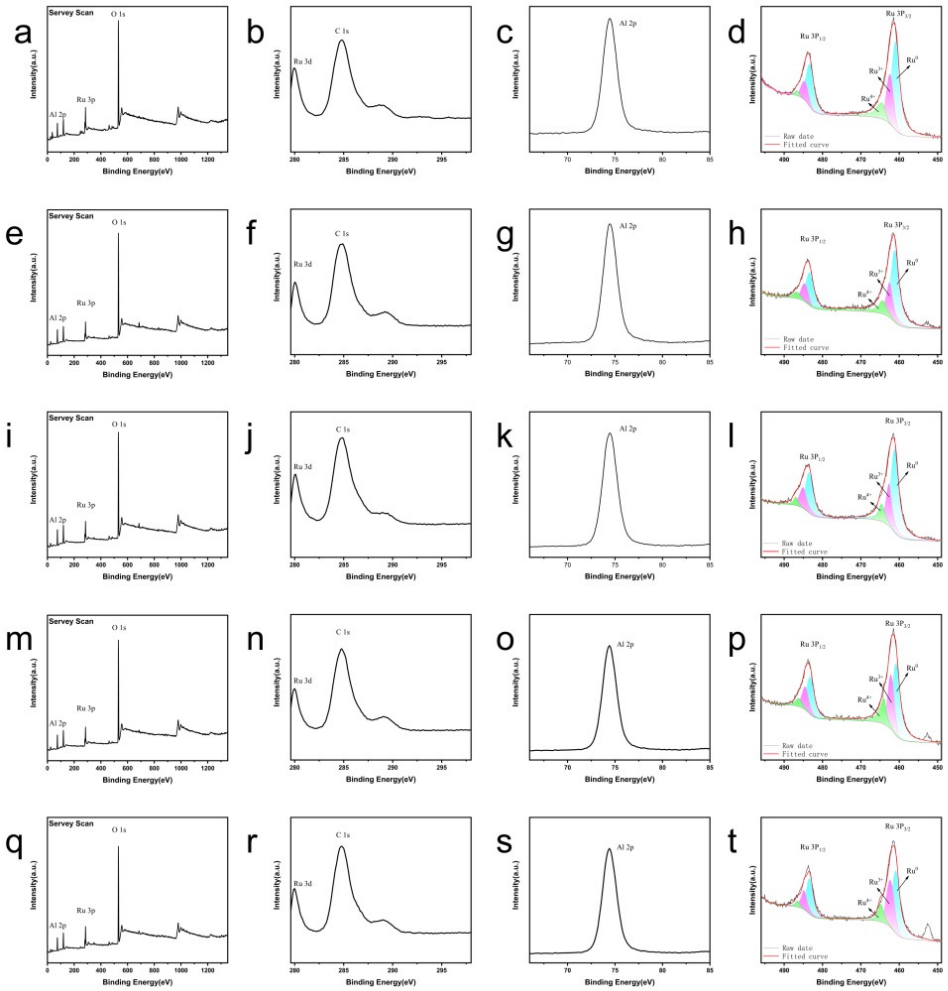

Figure S4. XPS spectra of the catalysts
(a-c) Ru/Al, (d-f) 2.5Li-Ru/Al, (g-i) 5Li-Ru/Al, (j-l) 7.5Li-Ru/Al, (m-o) 10Li-Ru/Al.

Table S2. Composition Analysis of Catalysts
(Determined by inductively coupled plasma optical emission spectrometry, ICP-OES)

Catalyst	Ru nominal (wt.%)	Ru actual (wt.%)	Li actual (wt.%)
Ru/Al	5.0	4.8	0
2.5Li-Ru/Al	5.0	4.9	0.5
5Li-Ru/Al	5.0	4.9	1.1
7.5Li-Ru/Al	5.0	5.0	1.4
10Li-Ru/Al	5.0	4.9	2.0

The ICP - OES analysis presented in Table 1 yields several significant insights into the catalyst composition. Notably, the Ru loadings were consistently maintained within the range of 4.8 - 5.0 wt.% regardless of the addition of Li. This consistency demonstrates the excellent retention of the active metal during the washing process. These results suggest that although the Ru loading was precisely controlled, the differences in catalytic performance observed among the samples likely originate from two factors: the deliberate variations in Li content (ranging from 0.5 - 2.0 wt.%) and potential interactions between Li and Ru, rather than from inadvertent compositional fluctuations. The high reproducibility of metal loadings, with an error margin of ±0.1 wt.%, validates the robustness of our preparation protocol.

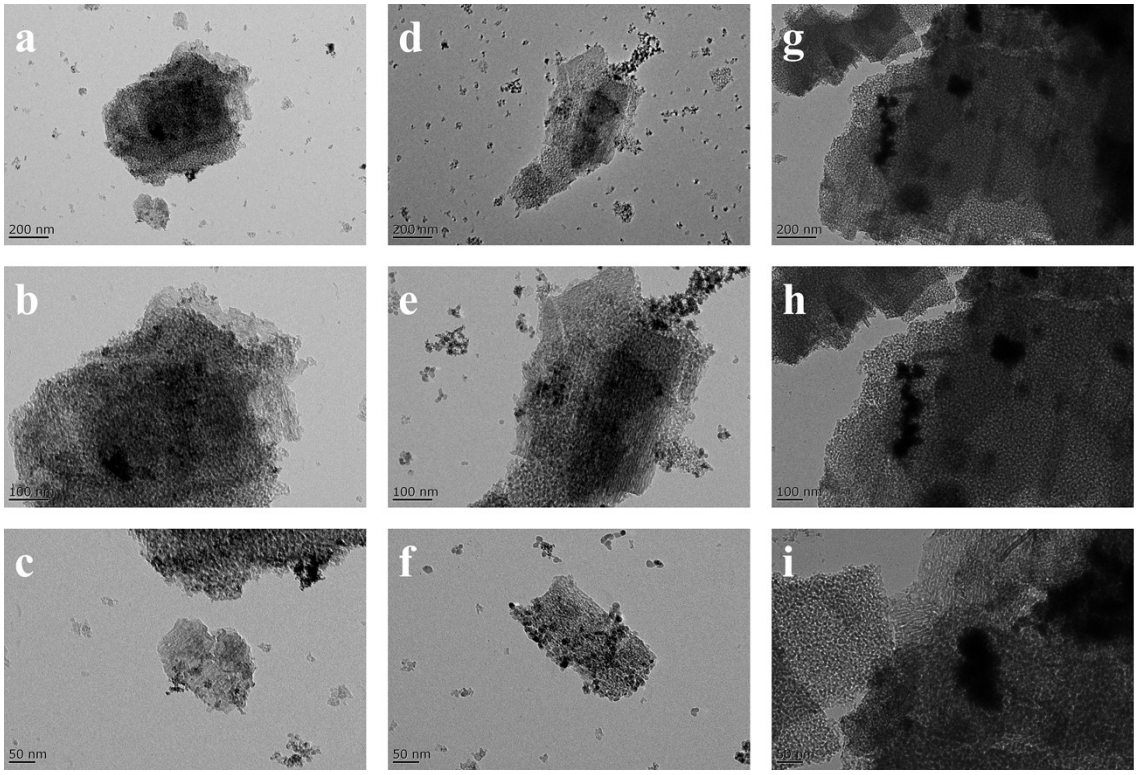

Figure S5. TEM Characterization of Recycled 5Li-Ru/Al Catalyst:
(a-c) Initial Catalyst (d-f) After 5 Cycles (g-i) After 10 Cycles

TEM analysis reveals that the deactivation of the recycled 5Li-Ru/Al catalyst is primarily attributed to the agglomeration of Ru nanoparticles. With increasing cycling numbers, Ru particles gradually grow and aggregate, reducing active sites and thus degrading catalytic performance.

Table S3. Variation of Metal Contents in 5Li-Ru/Al Catalyst During Cycling (ICP-OES)

Cycle number	Ru content (wt.%)	Li content (wt.%)	Ru retention (%)	Li retention (%)
Fresh	4.9	1.1	100	100
5 cycles	4.6	0.9	94	82
10 cycles	4.2	0.6	86	55

Characterization analysis indicates that the activity decline of the 5Li-Ru/Al catalyst is primarily caused by the agglomeration of Ru active species and the leaching of Li. The agglomeration of Ru reduces the number of active sites, while the loss of Li further contributes to the degradation of catalytic performance.